CONF-970604--42

# OXIDATION INDUCED STRESS-RUPTURE OF FIBER BUNDLES

**Edgar Lara-Curzio**
High Temperature Materials Laboratory
Oak Ridge National Laboratory
Oak Ridge, TN 37831

## ABSTRACT

The effect of oxidation on the stress-rupture behavior of fiber bundles was modeled. It is shown that oxidation-induced fiber strength degradation results in the delayed failure of the associated fiber bundle and that the fiber bundle strength decreases with time as $t^{-1/4}$. It is also shown that the temperature dependence of the bundle loss of strength reflects the thermal dependence of the mechanism controlling the oxidation of the fibers. The effect of gauge length on the fiber bundle strength was also analyzed. Numerical examples are presented for the special case of Nicalon™ fibers.

## NOMENCLATURE

| | | | | | |
|---|---|---|---|---|---|
| $a$ | defect size (m) | $h$ | gauge length (m) | $N_o$ | Original number of fibers |
| $A$ | area ($m^2$) | $k_l$ | parabolic rate constant ($m^2/s$) | $\sigma_b$ | bundle stress (Pa) |
| $\varepsilon$ | strain | $K_{IC}$ | stress intensity factor (Pa $m^{0.5}$) | $\Sigma_b$ | bundle strength (Pa) |
| $E$ | Young's modulus (Pa) | $\ell$ | fiber length (m) | $\sigma_o$ | characteristic strength (Pa) |
| $F$ | load (N) | $\ell_o$ | characteristic fiber length (m) | $t$ | time (hours) |
| $\Phi$ | probability of failure, fraction of failed fibers. | $m$ | Weibull modulus | $T$ | fiber stress (Pa) |
| | | $N$ | number of surviving fibers | $Y$ | geometric factor |

## 1. INTRODUCTION

The driving force behind the development of Continuous Fiber-reinforced Ceramic Composites (CFCCs) is the promise of substantial economic and environmental benefits if they are used in defense, energy and related industrial technologies, particularly at elevated temperatures [1]. The main attraction for using CFCCs over other high temperature materials, particularly monolithic ceramics, is their potential for superior toughness, tolerance to the presence of cracks and non-catastrophic mode of failure.

Since many of the potential applications for CFCCs involve components whose service lives are measured in tens of thousands of hours while subjected to relatively constant stresses [1], the successful design and implementation of CFCC components will depend on the availability of life-prediction methodologies and on knowledge of the evolution of the constituent properties over periods of time comparable to the expected service life of the component. For example, since the reliability and strength of CFCCs are primarily expected to be determined by the reliability and strength of the reinforcing fibers, it will be necessary to determine the time, stress, temperature and environmental dependence of fiber strengths, and accordingly, how these influence the reliability and strength of the component.

The need to know the evolution of fiber strength, for example, calls for methodologies for the mechanical characterization of fibers subjected to conditions similar to those that will be found in practice. Since single fiber testing can be tedious, alternative approaches may involve the evaluation of fiber bundles. This alternative approach becomes attractive because it reproduces the complex load history of a fiber when a composite is subjected to constant loading, although models of the mechanical behavior of fiber bundles will have to be available to interpret the experimental results. The complexity of the fiber load history arises from the fact that both the fiber strengths and fiber times-to-failure are statistically distributed, so that when a fiber fails, its load is redistributed to the surviving fibers in the fiber bundle.

Currently the performance of many non-oxide CFCCs is limited by the lack of environmentally stable fibers and fiber coatings, which makes necessary the investigation of environmental effects on the thermomechanical behavior of fibers. This paper analyzes the effect of oxidation on the stress-rupture behavior of fiber bundles.

The analysis presented here can be traced back to the work of Daniels, who developed a rigorous statistical theory for the relationships between tensile strength distributions for bundles and the constituent fibers [2]. In Daniels' model, the fibers are considered *classical* in the sense that their strength is independent of the rate of loading, have a known statistical distribution of strengths and follow equal load sharing, so that when one fiber of such bundle fails, it can not carry more load and its load is taken up equally by the surviving fibers. Coleman showed that when there is no dispersion in the fiber strength, then the bundle strength is the same as the fiber strength, but that as the coefficient of variation in fiber strength increases above zero the bundle strength approaches zero in the limit of infinite dispersion [3]. Coleman also developed statistical models to describe the mechanical breakdown of time-

dependent systems, such as fiber bundles, under different types of breakdown rules. He showed that under stress rupture conditions, for example, the lifetime of a fiber bundle is always shorter than the average lifetime of its component fibers [4]. Later on Phoenix and co-workers extended the work of Coleman by deriving rigorous analyses for the asymptotic time to failure of the fiber bundles subjected to different loading schedules [5]. In the next sections, an analysis is presented to determine the effect of oxidation on the stress-rupture behavior of fiber bundles composed of *classical* fibers. The special case of ceramic grade Nicalon™ fibers is considered.

## 2. ANALYSIS

Consider a bundle with a large but finite number of fibers of uniform cross-sectional area, $A$, that have the same linear stress-strain curve. If it is assumed that the strength-controlling flaws are restricted to the surface of the fibers, and that the strength of the fibers is described by a two-parameter Weibull distribution, then the probability of failure of the fibers when subjected to a uniform tensile stress $T$, will be given by

$$\Phi = 1 - exp\left\{-\frac{\ell}{\ell_o}\left(\frac{T}{\sigma_o}\right)^m\right\} \qquad (1)$$

where $\ell$ is the fiber length, $\sigma_o$ is the Weibull characteristic strength, and $m$ is the Weibull modulus. In this case, $\sigma_o$ is the stress required to cause on average, one failure in a fiber of length $\ell_o$ [6]. The Weibull modulus is a material constant that "measures" the variability in defect sizes, and henceforth, in strength. The probability of failure of the fibers will also equal the fraction of broken fibers in the bundle, i. e.

$$\Phi = 1 - \frac{N}{N_o} \qquad (2)$$

where $N$ is the number of unfractured fibers, and $N_o$ is the original number of fibers in the bundle. The bundle stress, $\sigma_b$, is defined as the ratio of the applied load, $F$, and the original cross-sectional area of the bundle, $N_oA$. By adopting a two-parameter Weibull distribution (Equation 1) to describe the distribution of fiber strengths, it is assumed that the threshold strength is zero, so that for $\sigma_b > 0$, the stress on each fiber will be always larger than the bundle stress. By considering a bundle in the Daniels sense, i. e. that the load applied to the bundle is equally distributed among the surviving fibers, the relationship between the applied load to the bundle, $F$, and the stress on each fiber, $T$, will be given by

$$T = \frac{F}{N_o\, A\, (1 - \Phi)} \qquad (3)$$

The so-called bundle-strength, $\Sigma_b$, given by the maximum load divided by the original cross-sectional area of the bundle can be determined by setting $dF/dT$, from Equation 3, equal to zero, which yields

$$F_{max} = N_o\, \sigma_o\, A \left(\frac{\ell}{\ell_o}\, m\, e\right)^{-\frac{1}{m}} \qquad (4)$$

and

$$\Sigma_b = \sigma_o \left(\frac{\ell}{\ell_o}\, m\, e\right)^{-\frac{1}{m}} \qquad (5)$$

although when the bundle reaches its strength, the stress acting on the unfractured fibers will be larger than the bundle strength and will equal

$$T_{max} = \sigma_o \left(\frac{\ell}{\ell_o}\, m\right)^{-\frac{1}{m}} \qquad (6)$$

Of practical interest in the experimental and analytical characterization of fiber bundles is their elongation as a function of time. In the case considered here of a bundle subjected to a constant bundle stress, $\sigma_b$, less than $\Sigma_b$, the elongation of the bundle will be given by

$$\varepsilon = \frac{F}{N\, A\, E} = \frac{T}{E} \qquad (7)$$

where $E$ is the elastic modulus of the fibers.

Consider a fiber bundle composed on non-interacting fibers, that is subjected to constant loading in air at a temperature at which the fibers do not flow (i. e. do not creep), but do oxidize[1]. For simplicity it is assumed that both the Weibull and Young's moduli of the fibers remain constant and that the only effect of oxidation is to decrease the characteristic strength of the fibers. In this case, the strength of the fibers will be controlled by surface defects resulting from oxidation, with the thickness of the oxide layer representing the size of the average strength-controlling flaw [7].

According to linear elastic fracture mechanics, the relationship between strength and flaw size is given by

$$K_{IC} = Y\, \sigma_o\, \sqrt{a} \qquad (8)$$

where $K_{IC}$ is the critical stress intensity factor, $Y$ is a geometric parameter, $\sigma_o$ is the strength and $a$ is the size of the strength-controlling flaw.

---

[1] It is assumed that the oxide scales do not bridge between fibers

# DISCLAIMER

Considering that the oxidation of most Si-based fibers is controlled by oxygen diffusion through the oxide layer, the oxide layer will grow according to:

$$\delta = \sqrt{k_1 t} \tag{9}$$

where $\delta$ is the thickness of the oxide layer at time t, and $k$ is the parabolic rate constant [8-9]. By assuming that the fracture toughness of the fibers remains constant, the combination of Equations 8 and 9 yields expressions for the time-dependency of the characteristic fiber strength:

$$\sigma_o(t) = \bar{\sigma}_o, \qquad t \le \frac{1}{k_1}\left(\frac{K_{IC}}{Y\,\bar{\sigma}_o}\right)^4$$
$$\sigma_o(t) = \frac{K_{IC}}{Y\sqrt[4]{k_1 t}}, \qquad t > \frac{1}{k_1}\left(\frac{K_{IC}}{Y\,\bar{\sigma}_o}\right)^4 \tag{10}$$

Equation 10 indicates that there exists an incubation period equal to the time required to grow an oxide layer as thick as the size of the average critical flaw in the unoxidized fibers[2]. Based on these and the considerations outlined above, both the deformation and strength of a fiber bundle subjected to constant loading can be determined as a function of time. This is described in the next section.

## 3. ALGORITHM

Except for a small number of values of $m$, this algorithm is based on the numerical solution of the iterated function system (IFS) formed by Equations 1 and 3. Despite its simplicity, a description of the algorithm is presented here because it reflects physical aspects of the problem which are intrinsic to the mechanics of deformation of fiber bundles.

Assume that the fiber bundle is subjected to a constant tensile load, $F$. For this load, and the corresponding bundle stress, a value for the fiber stress, $T$, can be obtained from Equation 3, assuming that all the fibers are intact ($\Phi = 0$). However, once the load is applied, some fibers will fail due to their statistical distribution of strengths, and the number of failed fibers can be determined from Equation 1 for that value of $T$. With the number of failed fibers at the stress $T$ just found, a new value of $T$ is calculated using Equation 3, because according to the global load sharing assumption, the load applied to the fiber bundle is redistributed among the surviving fibers. Then, a new probability of failure is calculated using Equation 1, and the process is repeated until:

1. The IFS settles at an attractor, which means that there exists a value of $T$ that satisfies simultaneously both Equations 1 and 3, ($\sigma_b < \Sigma_b$,) or
2. The IFS diverges, ($\sigma_b \ge \Sigma_b$).

If the bundle load is applied instantaneously, then the process described by the algorithm also occurs instantaneously. The existence of an attractor indicates that the fiber bundle reaches an equilibrium point so that the surviving fibers are capable of bearing the applied load, otherwise, the divergence of the IFS indicates the failure of the fiber bundle.

Although a fiber bundle may survive the initial application of the load, the oxidation of the fibers will initiate a process that will ultimately lead to the failure of the fiber bundle. The elongation, fiber loading history and the life of the fiber bundle under consideration are determined as follows: At a given time after the elapse of a time interval $\Delta t$, $0 \le t + \Delta t \le t_f$, the average thickness of the fiber oxide layer is determined using Equation 9, and the characteristic strength is modified according to Equation 10. Then the algorithm described above is repeated, resulting in either a new equilibrium point, or the divergence of the IFS reflecting the failure of the fiber bundle. This process can be visualized by considering that changes in the characteristic strength of the fibers result in the translation of the curves associated with Equations 1 and 3 in the $\Phi$-$T$ space [10]. As long as these curves intersect, meaning that there exists an attractor for the IFS, the fiber bundle can bear the applied load, otherwise, the inexistence of an intersection point symbolizes the failure of the fiber bundle.

## 4. RESULTS AND DISCUSSION

Using the numerical values given in Table I, stress and strain histories were generated for a hypothetical bundle of ceramic grade Nicalon™ fiber. Figure 1 shows the results at three different temperatures from fiber bundles subjected to a constant fiber bundle stress of 500 MPa that was applied instantaneously such as during a stress-rupture test. During the incubation period, explained in relation to Equation 10 in Section 2, neither the bundle strain or the fiber stress change with time. The duration of this incubation period is inversely proportional to temperature, in accordance to the thermally activated nature of the fiber oxidation process. Although the applied bundle stress is 500 MPa, the fiber stress at time zero is 512 MPa, because based on the numerical values used, and the explanation provided in Section 3, a small number of fibers will fail (2.4%) upon the application of the load, as shown in Figure 2. Note in Figure 1 that at the end of the incubation period, both the bundle strain and the fiber stress increase nonlinearly with time, and the arrows indicate the occurrence of the bundle failure. This portion of the curves represents a regime of accelerated deformation in which the effective load-bearing area of the bundle decreases with time as a result of fiber failure. This is analogous to the necking process exhibited by metals during creep. The shape of the strain versus time curves shown in Figure 1 is also similar to that exhibited by some CFCCs when subjected to stress-rupture conditions [11].

[2] It is usually found that at short oxidation times the strength of SiC increases because the oxide layer heals surface defects. However, at longer times, oxidation results in strength reduction. Here it is assumed that the strength of the fibers remains constant until the oxide layer becomes larger than the critical defect size associated with the characteristic strength of the original unoxidized fiber strength distribution.

Note that because the fiber's Young's modulus is assumed to be constant with temperature, the three curves start at the same strain value. The results in Figure 1 show, as expected, that the time-to-failure of the fiber bundle increases with decreasing temperature. Furthermore, it is illustrative to observe that although the force applied to the bundle is kept constant during the test, the stress in the fibers increases with time, consistent with the global load sharing assumptions. The reader is reminded that no effects, other than oxidation, have been considered in the analysis, and that the elongation of the bundle with time results from a collective structural breakdown process, and not from material flow.

Figure 2 shows the evolution of the probability of failure, or fraction of failed fibers as a function of time. It is interesting to observe that for the cases analyzed here, it only requires the failure of a relatively small fraction of fibers (≈ 20 %) to result in the failure of the fiber bundle. Also notice that the fraction of fractured fibers that triggers this *snow-ball* effect resulting in the failure of the fiber bundle increases with decreasing temperature. By plotting the time-to-failure as a function of temperature, using an Arrhenius plot (Figure 3) we find that the temperature dependence of the failure times coincides with that of the oxidation of the fibers.

The stress-dependence of both the fiber bundle strain and fiber stress histories is shown in Figure 4. Figure 4 shows curves generated at a temperature of 900°C for three different bundle stresses. Note that in this case the curves start at different strain levels, but that the duration of the incubation period is the same since its duration only depends on temperature. It can be observed that the rate of deformation increases with the fiber bundle stress, and that the life of the bundle decreases with increasing fiber bundle stresses. Using the results in Figure 4 and plotting the fiber bundle strength vs. the time-to-failure, as indicated in Figure 5, it can be observed that the time dependence of the fiber bundle strength is

$$\Sigma_b(t) \approx t^{-\frac{1}{4}} \qquad (11)$$

consistent with the time dependence of the characteristic strength of the fiber strength distribution, as indicated by Equation 10. Also in Figure 5 the effect of gauge length on the strength of the fiber bundle is illustrated. The results in Figure 5 indicate that the fiber bundle strength is higher for shorter bundles, or in other words, that shorter fiber bundles are more durable than longer fiber bundles, in agreement with the assumptions of the statistical distribution of defects and strengths. This dependency was already described by Equation 5, and it is shown graphically by Figure 6. This aspect of the analysis is important because in actual components, the effective gauge length of the fiber bundles will be much shorter than what is typically evaluated in the laboratory.

It should be indicated that the time-dependent elongation of the fiber bundles, as described in this paper, arises only from the collective breakdown of the bundle and not from material flow (i.e. creep). Therefore, it is likely that the "stress-relaxation" of SiC yarns that had been reported at room temperature can be explained using the concepts presented in this paper instead of the assumed viscoelastic behavior of the material [12].

## 5. CONCLUSIONS

Using a simple analysis, the effect of fiber oxidation on the stress-rupture behavior of fiber bundles was determined. It was found for the particular case in which the fibers oxidize and do not flow and/or exhibit fatigue effects, that the life of the fiber bundle decreases with increasing temperature and stress. It was also found that the thermal dependence of the fiber bundle failure times was the same as that of the fiber oxidation process, whereas the time-dependence of the fiber bundle strength was proportional to $t^{-1/4}$. Gauge length effects were also discussed, and it was shown that shorter fiber bundles are stronger and more durable than longer fiber bundles. This type of analysis will be useful to interpret experimental data generated from the evaluation of fiber bundles.

## 6. ACKNOWLEDGMENTS

This research was sponsored by the U. S. Department of Energy, Assistant Secretary for Energy Efficiency and Renewable Energy, Office of Industrial Technologies, Industrial Energy Efficiency Division and Continuous Fiber Ceramic Composites Program, under contract DE-AC05-96OR22464 with Lockheed Martin Energy Research Corp. The author is grateful to Matt Ferber of ORNL for very stimulating discussions, and to H. T. Lin and K. Breder of ORNL for reviewing the manuscript.

## 7. REFERENCES

1. M. A. Karnitz, D. F. Craig and S. L. Richlen, "Continuous Fiber Ceramic Composite Program," *Ceramic Bulletin*, **70**, (1991) 430-5
2. H. E. Daniels, "The Statistical Theory of the Strength of Bundles of Threads. I," *Proc. R. Soc. London*, **A183**, pp.405-35 (1944)
3. B. D. Coleman, "On the Strength of Classical Fibers and Fiber Bundles," *J. Mech. Phys. Solids*, **7**, (1958) pp. 60-70
4. B. D. Coleman, "Statistics and Time Dependence of Mechanical Breakdown in Fiber," *J. Appl. Phys.* **29**, 6, (1958) 968-983
5. S. L. Phoenix, "Stochastic Strength and Fatigue of Fiber Bundles," *Intl. Journ. of Fracture*, **14** (1978) 327-344
6. W. A. Curtin, "Theory of Mechanical Properties of Ceramic Matrix Composites," *J. Amer. Ceram. Soc.*, **74** [11] 2387-45 (1991)
7. A. Helmer, H. Peterlik, and K. Kromp, "Coating of Carbon Fibers," *J. Am. Ceram. Soc.*, **78** [1] pp. 133-36 (1995)
8. L. Filipuzzi, and R. Naslain, "Oxidation Mechanisms and Kinetics of 1-D SiC/C/SiC Composite Materials: II, Modeling," *J. Amer. Ceram. Soc.*, **77** [2] 467-80 (1994)
9. L. Filipuzzi and R. Naslain, "Oxidation Kinetics of SiC-Based Ceramic Fibers," Advanced Structural Inorganic Composites, P. Vincenzini, Ed. Elsevier Science Publishers, (1991) pp. 35-46

10. E. Lara-Curzio, M. K. Ferber and P. F. Tortorelli, "Interface Oxidation and Stress-rupture of Nicalon™/SiC CFCCs at Intermediate Temperatures," *Key Engineering Materials*, Vols. **127-131** (1997) pp. 1069-1082
11. E. Lara-Curzio and M. K. Ferber, "Stress Rupture of Nicalon™/SiC CFCCs at Intermediate Temperatures," *J. Mater. Sci. Letters*, **16**, 1 (1997) pp.23-26
12. F. Fang, F. Ko, C. Pastore and M. Koczak, "Stress-Strain-Time Relationship of SiC Yarns," Proc. Intl. Symp. on Composite Matls. and Structures, Beijing, China, June 10-13, 1986

Table I. Numerical constants used in the calculations. These values are representative of ceramic grade Nicalon™ fibers

| | |
|---|---|
| $E$ | 200 GPa |
| $h$ | 0.25 m |
| $K_{IC}$ | 0.8 MPa $m^{0.5}$ |
| $m$ | 3.8 |
| $\sigma_o$ | 1.8 GPa |
| $k_1$ | exp(11.34 - 8,887/T) $nm^2$/min |

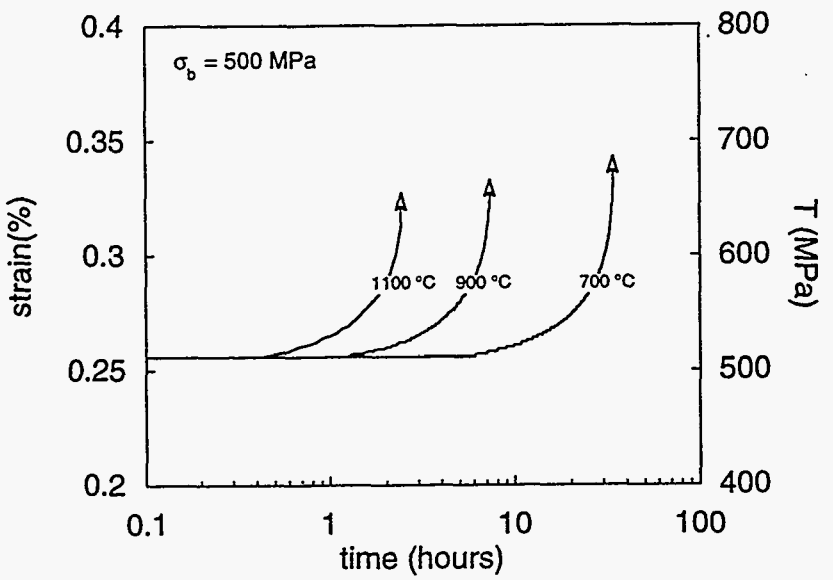


Figure 1. Strain and fiber stress histories for fiber bundles subjected to a constant fiber bundle stress of 500 MPa. Results are presented for three different temperatures. The arrows indicate the failure of the fiber bundles.

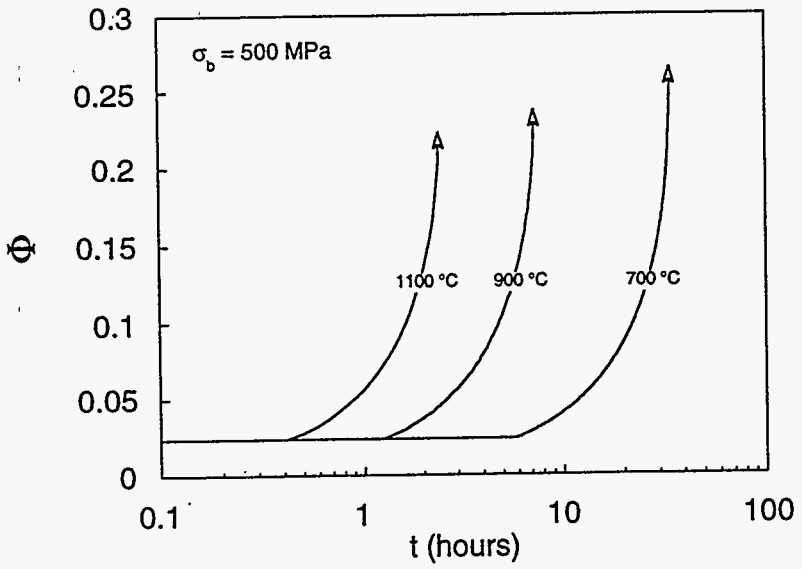


Figure 2. Evolution of the fiber probability of failure (or fraction of failed fibers) for a fiber bundle subjected to a constant fiber bundle stress of 500 MPa. Results are presented for three different temperatures. The arrows indicate the failure of the fiber bundles.

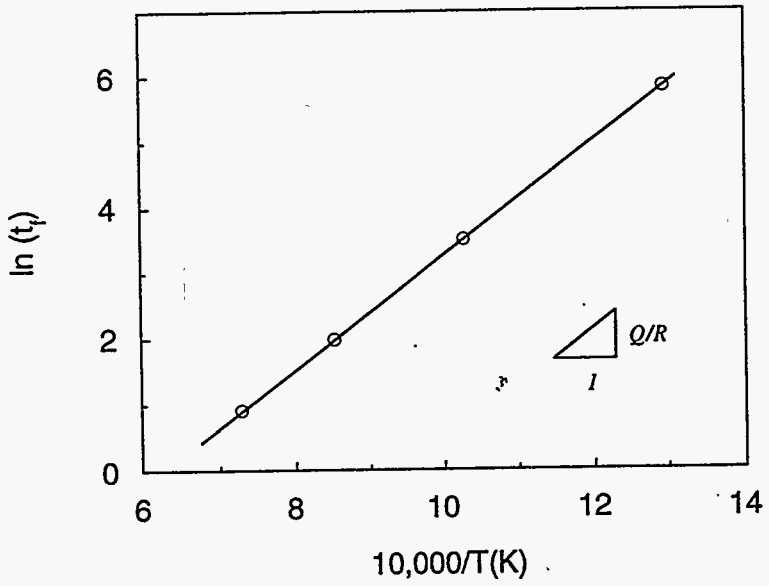


Figure 3. Arrhenius plot of the time to failure (in hours) for fiber bundles subjected to a constant fiber bundle stress of 500 MPa. The activation energy is that of the oxidation of the fibers.

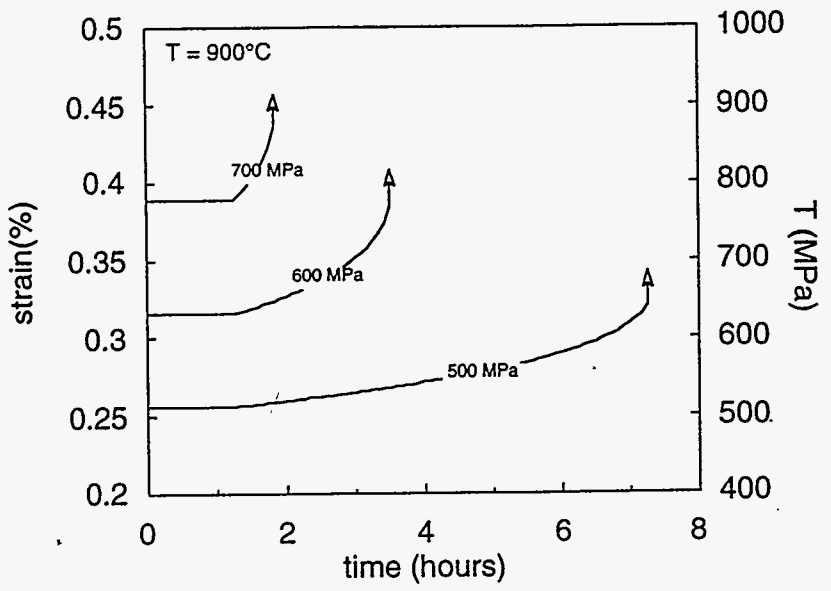


Figure 4. Strain and fiber stress histories for fiber bundles subjected to different constant fiber bundle stresses at 900°C. The arrows indicate the failure of the fiber bundles.

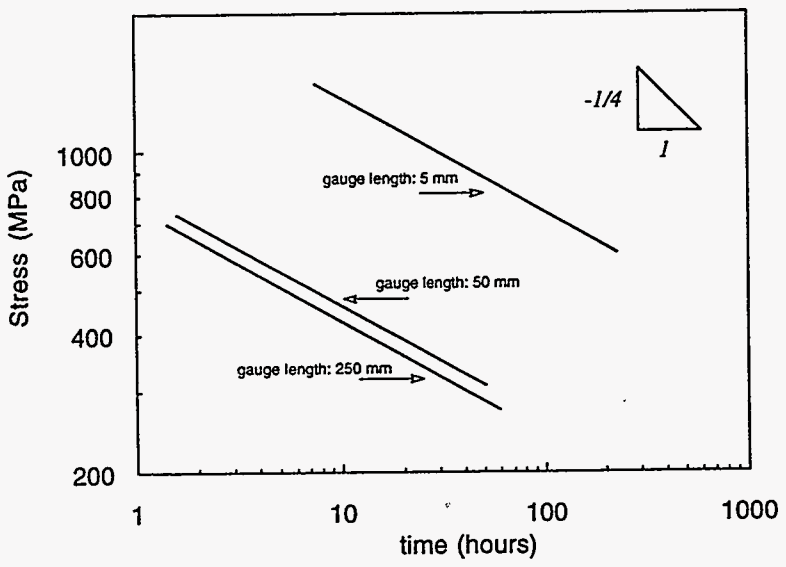


Figure 5. Gauge length effect on the time-dependency of the fiber bundle strength.

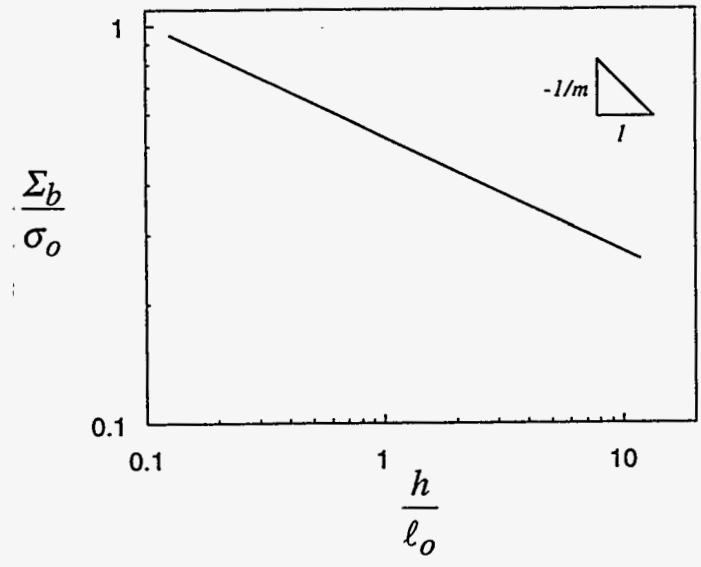


Figure 6. Gauge-length dependence of the fiber bundle strength, according to Equation 5.